A Comparative Study of CO Chemisorption on Al_2O_3 and Ti_2O_3 Nonpolar Surfaces

Maurizio Casarin,*,† Chiara Maccato,† and Andrea Vittadini‡

Dipartimento di Chimica Inorganica, Metallorganica ed Analitica, Università di Padova, 35131 Padova, Italy, and Centro di Studio della Stabilità e Reattività dei Composti di Coordinazione, CNR, 35131 Padova, Italy

Received: March 27, 2001; In Final Form: September 26, 2001

Density functional molecular cluster calculations have been used to investigate the interaction of CO with the $M_2O_3(10\bar{1}2)$ (M = Al and Ti) nonpolar surface. The electronic structure of the clean surface, the adsorbate geometry, vibrational parameters, and chemisorption enthalpies are computed and discussed. Theoretical results pertaining to the clean surface agree quite well with experimental measurements and other theoretical investigations. As far as the adsorbate−substrate interaction is concerned, our data indicate that the CO−$M_2O_3(10\bar{1}2)$ bonding is charaterized, in both Al_2O_3 and Ti_2O_3, by a two-way electron flow involving both donation from CO based σ levels into virtual orbitals of the unsaturated surface Lewis acid site and back-donation from surface states into the CO π^* virtual levels. However, the nature of surface orbitals involved in back-donation and the concomitant effects on the adsorbate structure are very different in the two cases. CO is only slightly affected upon chemisorption on $Al_2O_3(10\bar{1}2)$, while perturbations induced into the CO electronic and molecular structure by the interaction with the $Ti_2O_3(10\bar{1}2)$ surface are very intense and, consistently with experimental data, the C−O bond becomes strongly weakened.

1. Introduction

Titanium-based materials are particularly interesting because of their applications in several technological processes ranging from photocatalysis[1] to the preparation of thin films highly corrosion resistant and well tolerated by the human body.[2] Among the several stable oxides that titanium, as both pure metal and alloy, forms spontaneously when exposed to air, water, or aqueous biological environments, titanium dioxide (TiO_2) is certainly the most studied.[3] Besides the interest for TiO_2, also titanium sesquioxide (Ti_2O_3) is attracting a growing attention[4] as a consequence of its peculiar electronic properties.[5]

In the Ti_2O_3 corundum structure, metal and oxide ions are 6- and 4-fold coordinated, respectively (see Figure 1);[6] i.e., each Ti atom formally shares three of its four valence electrons with six oxygen atoms, thus contributing with $^1/_2$e to each Ti−O bond, while O atoms participate with $^3/_2$e to the same interaction. The nearly octahedral coordination of oxide ions around Ti^{3+} cations splits the Ti 3d orbitals into t_{2g}-like and e_g-like sets, with the former set more stable than the latter;[7] moreover, the actual symmetry of the lattice further splits the t_{2g}-like levels into a_{1g} and e_g (hereafter, e_g^{π}) states. The singly occupied a_{1g} orbitals have a $3d_{z^2}$ character and the correct form to originate a direct bond between pairs of Ti atoms within the face-sharing TiO_6 octahedra occurring along the *c* axis of the corundum structure. In this regard, it is useful to remember that the Ti_2O_3 unit cell includes two different pairs of Ti nearest neighbors: one with a short Ti−Ti′ interatomic vector (2.582 Å) parallel to the *c* axis; the other with a longer Ti−Ti″ interatomic vector (2.994 Å) almost parallel to the (0001) basal plane (hexagonal notation, see Figure 1). States accounting for the direct Ti−Ti′ interaction constitute the Ti_2O_3 valence band maximum (VBM) that is separated by a small gap (∼0.1 eV at 300 K)[8] from the conduction band minimum (CBM), which, besides the e_g^{π} levels, includes the a_{1g}* orbitals (Ti−Ti′ antibonding) and the e_g-like states antibonding in nature with respect to the Ti−O interaction.

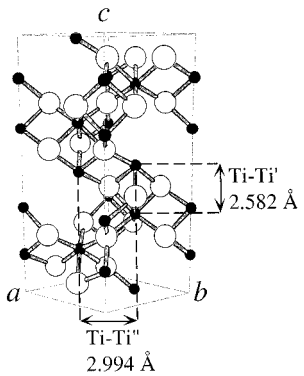

Figure 1. Side view of the Ti_2O_3 unit cell. Structural parameters are those of ref 6. Dark and white circles represent Ti and O atoms, respectively.

One-third of the possible octahedrally coordinated cation sites in the bulk corundum structure are vacant.[3] These vacancies are arranged on $(10\bar{1}2)$ planes, which are the primary cleavage plane for Ti_2O_3[9] but not for Al_2O_3. The perfect $M_2O_3(10\bar{1}2)$ surface is constituted by an equal number of cations and anions, each of them missing a single ligand (see Figure 2). The overall charge ($^1/_2$e) occupying the dangling bond (DB) of exposed M atoms of the second layer of the surface[11] can be thought to be transferred to the partially occupied DB of the topmost layer O atoms, which then becomes filled by two electrons. As a whole, the number of empty and filled DBs on the $M_2O_3(10\bar{1}2)$ is the same, and the surface is nonpolar. The properties of the clean $Ti_2O_3(10\bar{1}2)$[9] surface as well as its interaction with a series of simple inorganic molecules (O_2,[12a] CO,[12d] H_2O,[12b] SO_2,[12d]) have

* To whom correspondence should be addressed. Phone: 39-049-8275164. Fax: 39-49-8275161. E-mail: casarin@chin.unipd.it.
† Università di Padova.
‡ CNR di Padova.

10.1021/jp011140d CCC: $22.00
Published on Web 01/05/2002

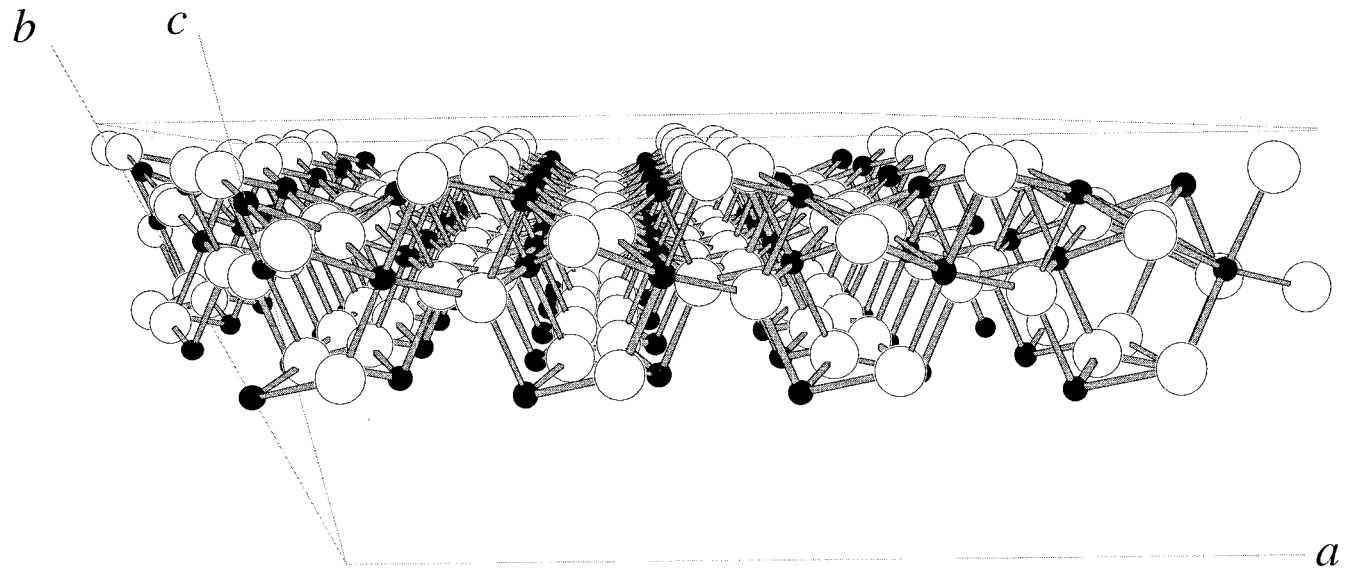

Figure 2. Model of the corundum ($10\bar{1}2$) surface. Exposed O and M atoms lie in the topmost and second layer, respectively. Both surface cations and anions carry a coordinative vacancy. The former are surrounded by five nearest-neighbor ligands (two in the topmost layer, two in the third layer, and one in the fifth); the latter are bonded to three M atoms (two in the second layer and one in the forth).

been thoroughly investigated by the Henrich group[12] by using several spectroscopic techniques; nevertheless, no theoretical contribution has been dedicated to this issue to our knowledge.

We already showed that small clusters terminated with pseudo-hydrogens are able to model adequately the molecular adsorption of simple molecules (CO, NH_3, H_2O, H_2S, CH_3OH, CH_3SH) on ionic material surfaces.[13] As a part of an ongoing research program devoted to the investigation of the surface reactivity of metal oxides, in the near past we theoretically explored the molecular chemisorption of CO on the nonpolar α-$Al_2O_3(0001)$ surface[13g,14] by coupling the molecular cluster approach to the density functional theory (DFT). We found that (i) the most stable CO chemisorption geometry ($\Delta H_{ads} \sim -13$ kcal/mol) is that corresponding to the adsorbate perpendicular to the surface, atop the Lewis acid site (L_s^a) and C-down oriented, (ii) the C−O stretching frequency (ν_{C-O}) computed for such an arrangement is 2158 cm^{-1}, i.e., blue shifted by 44 cm^{-1} with respect to the one computed for the free adsorbate, and (iii) the adsorbate−substrate interaction relieves some of the L_s^a relaxation, even if the L_s^a electronic structure is only slightly affected upon chemisorption.

In the present contribution we present the results of a theoretical study concerning the bonding of CO to the $M_2O_3(10\bar{1}2)$ (M = Al, Ti) nonpolar surface to look into the role played by the 3d electrons in the CO chemisorption process on passing from Al_2O_3 to Ti_2O_3 as well as to investigate if the chemisorption process affects the direct Ti−Ti′ bond.

2. Computational Method

2.1. Models. We have considered several model clusters (some of them are displayed in Figure 3) as representative of the M_2O_3 bulk phase (model **B**, where each M atom is surrounded by the atoms belonging to the three nearest neighbor spheres: a sphere of M atoms and two spheres of O atoms) and its nonpolar ($10\bar{1}2$) surface (models **S1**, **S2**, and **S3** the top side of which mimics the surface). The experimental lattice constants of Al_2O_3 ($a = b = 4.7570$ Å, $c = 12.9877$ Å)[16] and Ti_2O_3 ($a = b = 5.157$ Å, $c = 13.610$ Å)[6] have been adopted for calculations. Spurious surface states have been avoided by saturating DBs of atoms not chemically complete[17] with pseudo-hydrogen saturators carrying a fractional nuclear charge. It can be useful to remember that such a procedure has been successfully applied to model metal oxide surfaces including $TiO_2(110)$[13e] and α-$Al_2O_3(0001)$.[13g] The settling of pseudo-hydrogen nuclear charge is based on the number of electrons shared by M and O atoms (see above). According to that, model clusters have been saturated by providing $^3/_2$ and $^1/_2$ electrons to each M and O DB, respectively. This result can be obtained by employing saturators with $Z = {}^1/_2$ (H′) and $Z = {}^3/_2$ (H″). In the present contribution all the model clusters have no peripheral

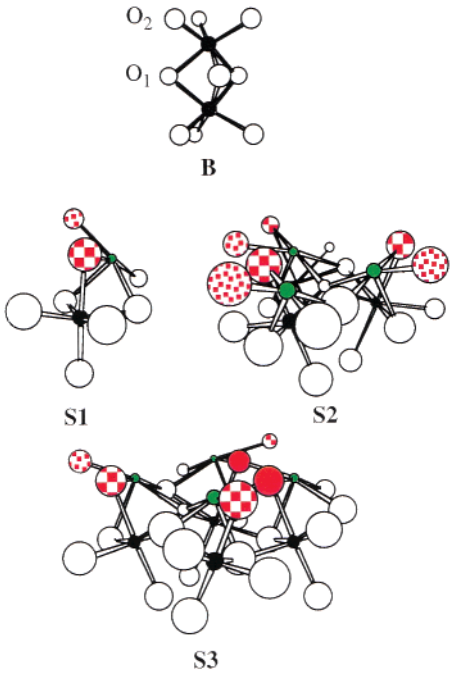

Figure 3. Schematic structure of the model clusters adopted to represent the M_2O_3 bulk phase (**B**) and the $M_2O_3(10\bar{1}2)$ surface (**S1**, **S2**, and **S3**). Green and red circles refer to surface, chemically complete L_s^a and L_s^b, respectively, while checkered and pied circles indicate surface O atoms saturated with one or two saturators, respectively. Pseudo-atoms are not included in the figure for the sake of clarity.

cations, thus avoiding the use of H″ saturators. All H′ pseudo-atoms have been placed along the bond directions of the extended lattice; moreover, the optimal O−H′ (1.055 Å) bond length (BL) was determined by minimizing the total energy of the tetrahedral OH'_4 pseudo-molecule.

At variance to the actual $(10\bar{1}2)$ surface, model clusters **S1**, **S2**, and **S3** do not contain an equal number of surface L_s^a and Lewis base sites (L_s^b). More specifically, **S1**, **S2**, and **S3** include one, three, and four L_s^a, respectively (see Figure 3), while **S1** has two L_s^b and both **S2** and **S3** hold six of them. This generates a defect of electrons in the surface states that could be corrected by imposing ad hoc electrostatic net charges to the clusters. In detail, the following charges should be imposed to **S1**, **S2**, and **S3**: $-1/2$, $-3/2$, and -1, respectively. In the present case, rather than employing charged clusters, we preferred to use an alternative approach already adopted to simulate $TiO_2(110)$[13e] and α-$Al_2O_3(0001)$[13g] surfaces. Actually, replacing the three H′ saturators of the surface L_s^b of **S1** (see Figure 3) with three pseudo-atoms having $Z = 2/3$ implies the introduction of $1/2$ excess electrons in the cluster levels. Moving to **S2** and **S3**, among the six surface L_s^b of **S2** (**S3**), three (two) of them (see Figure 3) need only one saturator; the saturation of these oxygens with hydrogen atoms rather than with H′ adds just $3/2$ (1.0) excess electrons in the cluster levels. We already showed in refs 13e and 13g that this procedure is preferable because no arbitrary shifts are needed to compare one-electron energy levels.

2.2. Computational Details. All the calculations have been run within the density functional theory (DFT) approach by using the ADF 1999 package.[18,19] Geometry optimization, binding energies, and vibrational frequencies were obtained by using generalized gradient (GGA) corrections self-consistently included through the Becke−Perdew (BP) formula.[20] As a matter of fact, BP GGAs are able to significantly improve the agreement of metal−ligand binding energies[21] and of adsorption energies[22] with experimental data.

A triple-ζ Slater-type basis set was used for Ti, Al, and O and C atoms of CO, while for the substrate O atoms and saturators (pseudo-hydrogen and hydrogen atoms) we used a double-ζ basis. The inner cores of Ti (1s2s2p), Al (1s2s2p), and O (1s) and C (1s) atoms were treated by the frozen-core approximation.

The adsorption enthalpy (ΔH_{ads}) was analyzed in terms of the adsorbate and substrate fragment orbitals by applying Ziegler's extended transition state method[23] (ETS). According to the ETS scheme, ΔH_{ads} can be written as

$$\Delta H_{ads} = \Delta E_{elstat} + \Delta E_{Pauli} + \Delta E_{int} + \Delta E_{prep}$$

Here, ΔE_{elstat} is the pure electrostatic interaction, ΔE_{Pauli} is the destabilizing two-orbital−four-electron interaction between the occupied orbitals of the two fragments, ΔE_{int} derives from the stabilizing interaction between occupied and empty orbitals of the interacting fragments, and the last term ΔE_{prep} provides information about the energy required to relax the structure of the free fragments to the geometry they assumed in the final system.

Final adsorption enthalpies were further corrected by taking into account the basis set superposition error (BSSE), which was estimated through the use of reference energies computed with ghost adsorbate and surface fragments.[24]

Density of states (DOS), partial density of states (PDOS), and crystal orbital overlap population (COOP)[25] curves have been computed by applying a Lorentzian broadening of 0.25 eV to the eigenvalues of the clusters. Both PDOS and COOP curves were obtained by weighting one-electron energy levels by their basis orbital percentage, so providing information about the localization and the bonding/antibonding character of selected molecular orbitals (MOs).

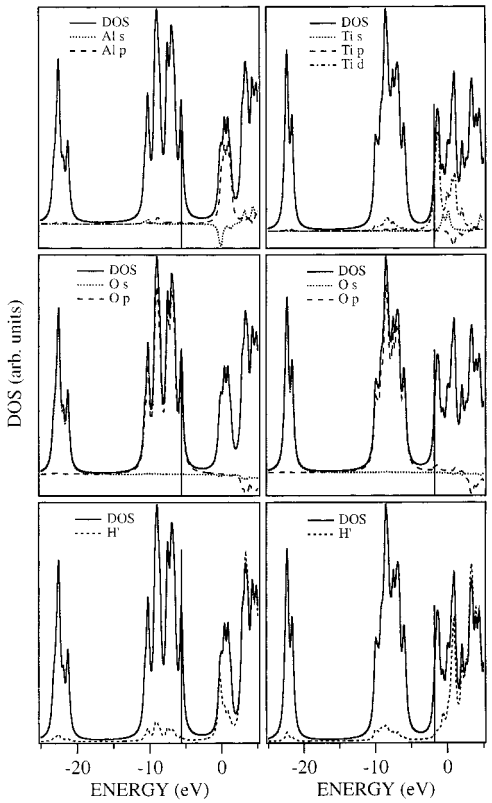

Figure 4. DOS of the ^{Al_2O_3}**B** (left) and ^{Ti_2O_3}**B** (right) model clusters. PDOS of M, O, and saturators are also displayed. Vertical bars represent the energy of the highest occupied MO (HOMO).

3. Results and Discussion

3.1. Bulk Phase. Results pertaining to ^{Al_2O_3}**B**[26] are not particularly surprising. Actually, the corresponding DOS curves in the energy region including occupied levels consist of two broad bands centered at ∼−22 and ∼−9 eV (see Figure 4). The former includes O 2s atomic orbitals (AOs), while the latter is mainly due to MOs having a significant participation of the O 2p AOs. The width of the O 2s and O 2p valence bands are 2 and 5 eV, respectively, in reasonable agreement with Discrete variational (DV) Xα results reported by Guo et al.[29] for an 80 atom cluster embedded in the infinite host lattice and having ^{Al_2O_3}**B** as the inner core. Furthermore, the ^{Al_2O_3}**B** lowest unoccupied MO (LUMO), somehow representative of the CBM, is strongly localized on the Al 3s AOs, and the HOMO−LUMO gap is 5.30 eV. In this regard, it has to be noted that the energy gap computed by Guo et al.[29] is 11.4 eV while the experimental one[30] is 9.2 eV. As far as the Al and O effective atomic charges are concerned, the values obtained from the Mulliken population analysis[31] are +1.91 and −1.28/−1.23,[32] respectively, i.e., definitely smaller than those reported by Guo et al.[29] (+2.93 and −1.95 for Al and O, respectively). A further point deserving to be stressed concerns the low contribution provided to the occupied DOS by saturators, which confirms that H′ pseudo-atoms are well suited for their purpose.

The ^{Ti_2O_3}**B** DOS curves obtained from non-spin-polarized calculations are also displayed in Figure 4. The main difference with the ^{Al_2O_3}**B** DOS is related to the position and the nature of the HOMO, now localized on the Ti 3d AOs and accounting

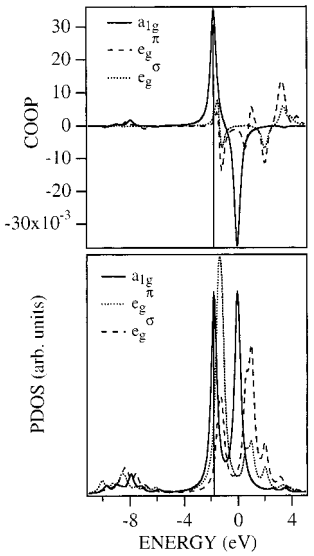

Figure 5. Ti−Ti′ COOP (up) and Ti PDOS (down) in ^{Ti_2O_3}**B**. Bonding and antibonding states correspond to COOP positive and negative peaks, respectively. Vertical bars represent the energy of the HOMO.

for a direct (ddσ)−type bonding between titanium atoms (see Figure 5). Furthermore, according to experimental results,[12d] theoretical calculations predict a ΔE of ∼4 eV between the MO accounting for the direct Ti−Ti′ σ bond and the top of the O 2p band, whose width is ∼5 eV. In this regard, it is of some relevance to mention that the metallic behavior that could be attributed to Ti_2O_3 by the analysis of Figure 4 is only an artifact of the procedure we adopted to broaden the one electron energy levels of the model cluster. As a matter of fact, the inspection of Figure 5, where the PDOS of Ti 3d orbitals is reported, allows us to appreciate a HOMO−LUMO ΔE of ∼0.3 eV. Moreover, as already found for ^{Al_2O_3}**B**, the contribution provided by pseudo-atom saturators to the outermost occupied DOS is negligible.

As far as the Ti and O effective atomic charges are concerned, the computed values (+1.72 and −1.18/−1.27 for Ti and O_1/O_2, respectively) are slightly smaller than those obtained for ^{Al_2O_3}**B** (see above), indicating a more covalent nature of Ti_2O_3 with respect to Al_2O_3.

As a whole, these outcomes indicate that both ^{Al_2O_3}**B** and ^{Ti_2O_3}**B** clusters, despite their very limited size, are able to reasonably reproduce the main features of the M_2O_3 electronic structure.

3.2. Clean Surface. Theoretical calculations pertaining to the clean $M_2O_3(10\bar{1}2)$, as well as to the surface interacting with CO, have been carried out by freezing the coordinates of the substrate atoms.[33] The DOS/PDOS of **S1**, **S2**, and **S3** are displayed in Figure 6, while in Table 1 the effective atomic charges of atoms representative of the surface or having a complete shell of nearest neighbors are reported. We first note that, in both Al_2O_3 and Ti_2O_3, the main features of the DOS of the $(10\bar{1}2)$ surface are scarcely affected by the cluster size. Moreover, the inspection of Figure 6 indicates that the ^{Al_2O_3}**S3** VBM (CBM) is mainly due to 2p (3s) states localized on O (Al) surface atoms (O_s and Al_s, respectively). Such a result is well in tune with DV-Xα outcomes reported by Guo et al.[34] in their study devoted to the electronic structure and the energetics of sapphire (0001) and $(1\bar{1}02)$ surfaces.[35] In this regard, it has to be also pointed out that (i) in agreement with data of Guo et al.,[34] the charge of surface atoms (see Table 1) is smaller (in absolute value) than that localized on atoms belonging to inner layers, and (ii) analogously to the results pertaining to the bulk (see above), the absolute values of the effective atomic charges

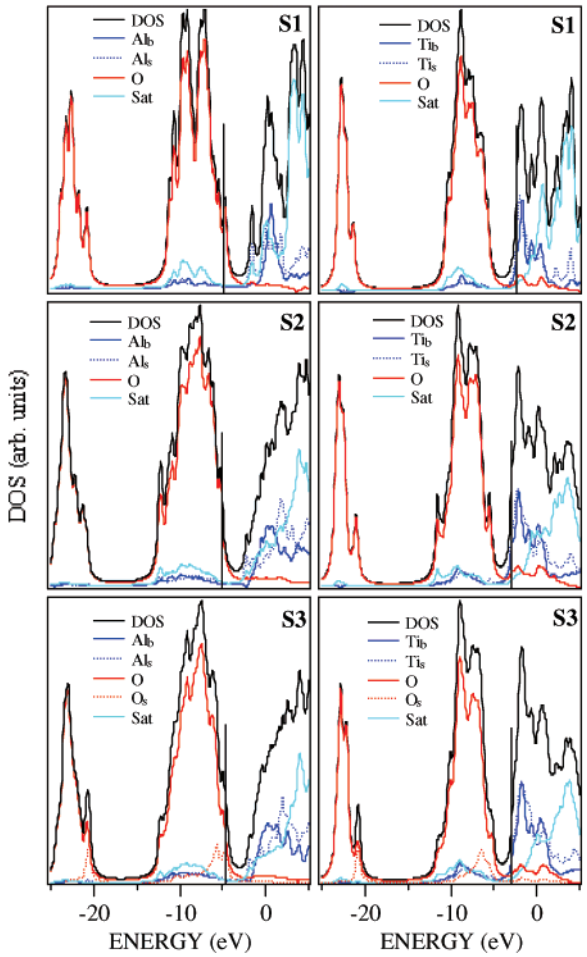

Figure 6. DOS of the ^{M_2O_3}**S1**, ^{M_2O_3}**S2**, and ^{M_2O_3}**S3** model clusters. PDOS of M, O, and saturators are also displayed. Vertical bars represent the energy of the highest occupied MO (HOMO).

TABLE 1: Gross Mulliken Charges of Surface (s) and "bulk" (b) Atoms

	^{Al_2O_3}**S1**/^{Ti_2O_3}**S1**	^{Al_2O_3}**S2**/^{Ti_2O_3}**S2**	^{Al_2O_3}**S3**/^{Ti_2O_3}**S3**
M_s	1.54/1.46	1.53[a]/1.46[a]	1.53[a]/1.46[a]
M_b	1.68/1.64	1.72[a]/1.57[a]	1.71[a]/1.56[a]
O_s			−1.03[a]/−0.92[a]
O_b		−1.09/−1.03	−1.10/−1.03

[a] Mean value.

deriving from our calculations are definitely smaller than those computed by Guo et al.[34]

Theoretical outcomes relative to the $Ti_2O_3(10\bar{1}2)$ surface substantially mirror those pertaining to the bulk phase. With reference to ^{Ti_2O_3}**S3**, the outermost four occupied MOs are grouped in an energy range of 0.2 eV, they are all localized on the $3d_{z^2}$ AO of the eight Ti atoms of the model cluster, and all of them have a Ti−Ti′ bonding character (see Figure 7). The top of the O 2p band lies at 2.5 eV below the innermost of the Ti−Ti′ bonding MOs, and according to the results of the Henrich group,[12] it extends for ∼6 eV. Furthermore, once again in agreement with UPS measurements of Smith and Henrich,[12d] the O 2p PDOS of both ^{Ti_2O_3}**S2** and ^{Ti_2O_3}**S3** are characterized by a double-peaked structure. The higher energy peak is due to nonbonding MOs (the threshold of the O 2p band is originated by the occupied O_s DBs), while the lower energy one includes bonding partners. Finally, analogously to the results obtained for **B**, the effective atomic charges reported in Table 1 indicate a higher covalency of Ti_2O_3 compared to Al_2O_3. In this regard,

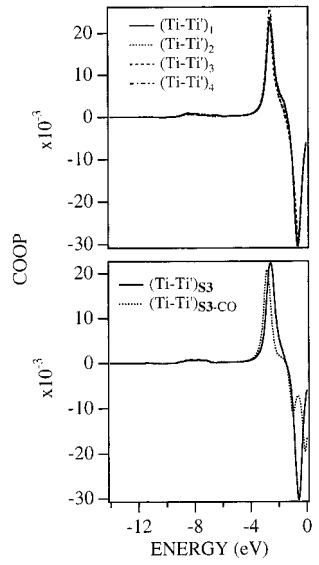

Figure 7. COOP between different Ti−Ti′ pairs in **S3** (up). COOP between $(L_s^a-Ti)_s$ in **S3** and **S3**−CO model clusters (down).

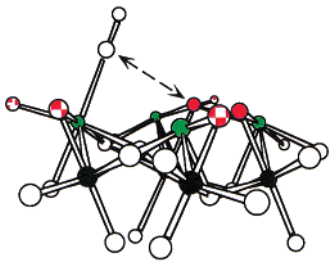

Figure 8. Schematic structure of the **S3** model cluster interacting with the CO molecule C-down oriented.

it is noteworthy that the effective charge of Ti_s (1.46, see Table 1) is very close to three-fourths the value we computed for Ti surface atoms of $TiO_2(110)$.[13e] This evidence indicates that the adopted clusters, despite their limited size, are able to reproduce satisfactorily the main features of the Al^{3+} and Ti^{3+} Lewis acid sites available on the $(10\bar{1}2)$ surface of Al_2O_3 and Ti_2O_3.

3.3. Molecular Adsorption of CO. The bonding between CO and the $M_2O_3(10\bar{1}2)$ surface has been investigated by allowing the interaction of the adsorbate C-down oriented[37] atop one of the L_s^a available on the substrate and limiting the optimization procedure to the adsorbate coordinates. For each substrate, theoretical outcomes computed for CO interacting with **S1**, **S2**, and **S3** are very similar and, for this reason, the forthcoming discussion will be limited to the analysis of data pertaining to ^{Al_2O_3}**S3**−CO and ^{Ti_2O_3}**S3**−CO model clusters (see Figure 8).

In Table 2 structural and vibrational parameters of CO in the free and adsorbed states are reported together with ΔH_{ads} values (see also Table 3). Starting with CO interacting with the $Al_2O_3(10\bar{1}2)$ surface, we remark that the optimized L_s^a−C BL (2.169 Å) is shorter than that computed by us for CO on α-$Al_2O_3(0001)$ (2.224 Å),[13g] and by Neyman et al.[38] (2.28/2.24 Å)[39] for a CO molecule bound to a five-coordinate Al^{3+} site in oxide systems. Furthermore, the L_s^a−C−O surface complex is significantly bent (the Al−$\hat{C}$−O bond angle (BA) is 170.2°). Finally, the C−O stretching frequency is almost unperturbed (red shifted by 4 cm^{-1}) upon coordination.[40]

As far as the ΔH_{ads} is concerned, our estimate of −12.23 kcal/mol is quite similar to the value (−13.36 kcal/mol) we computed for CO on α-$Al_2O_3(0001)$ but rather different from those reported by Neyman et al.[38] (−7.84/−8.53 kcal/mol). In this regard, it has to be remarked that (i) the cluster of C_{2v} symmetry adopted by Neyman et al.[38] as representative of a five-coordinate Al^{3+} site in oxide systems is very small ($Al(OH)_3(OH_2)_2$) and (ii) the $Al(OH)_3(OH_2)_2$ model cluster mimicked Al^{3+} species placed in the octahedral sites of the spinel structure, i.e., in a chemical environment completely different from the one herein considered.

TABLE 2: Structural and Vibrational Properties of the Free and Adsorbed CO As Obtained from GGA Calculations

	theor	exptl
^{free}CO		
r_{C-O} (Å)	1.140	1.127
ν_{C-O} (cm^{-1})	2114	2143
^{ads}CO		
	$Al_2O_3(10\bar{1}2)$	$Ti_2O_3(10\bar{1}2)$
r_{C-O} (Å)	1.139	1.158
$r_{L_s^a-C}$ (Å)	2.169	2.194
∠M−C−O (deg)	170.2	173.4
$\angle O_V$−M−C (deg)	170.3	178.2
ΔH_{ads} (kcal/mol)	−12.23	−16.10
ν_{C-O} (cm^{-1})	2110	1935
$\Delta\nu_{CO}$ (cm^{-1})	−4	−179

TABLE 3: Theoretical CO Adsorption Energies (kcal/mol) Decomposed by Means of the Ziegler Transition State Method

	^{Al_2O_3}**S3**−CO	^{Ti_2O_3}**S3**−CO
ΔE_{Pauli}	51.71	53.73
ΔE_{Elstat}	−35.11	−33.65
ΔE_{Int}	−30.08	−38.08
$\Delta E_{Prep,CO}$	0.00	0.42
BSSE	1.25	1.48
ΔH_{ads}	−12.23	−16.10

To our knowledge, only two experimental estimates of ΔH_{ads} of CO on Al_2O_3 (∼5[41] and ∼4 kcal/mol[42]) are present in the literature. The agreement with ΔH_{ads} = −12.23 kcal/mol is certainly poor; however, it deserves to be stressed that the former value has been indirectly obtained from IR measurements on powder samples,[41] while the latter refers to O-terminated epitaxially grown Al_2O_3 layers.[42,43] As a whole, both estimates are not well suited to be compared with the results of our calculations.

On passing from the free CO to the chemisorbed one, the adsorbate structure seems to be perturbed to a negligible extent. As a matter of fact, the adsorbate molecules carry a net positive charge ($Q = 0.04$)[44] less than one-third of the one we evaluated for CO on α-$Al_2O_3(0001)$, its stretching frequency is red shifted by only 4 cm^{-1}, and the C−O ΔBL upon chemisorption is negligible (note the zero value of the ΔE_{prep} in Table 2). Nevertheless, it deserves to be remarked that both the Al−$\hat{C}$−O and O_v−$\hat{A}$l−C[45] BAs differ significantly from 180° (170.2 and 170.3°, respectively). In relation to that, it may be useful to remember that Kettle[46] pointed out on the basis of symmetry arguments that deviations from linearity in terminal carbonyls are related to the different occupations of CO-based π^* orbitals. Obviously, the L_s^a available on the $Al_2O_3(10\bar{1}2)$ surface cannot be involved in any L_s^a→CO back-bonding interaction, but it is noteworthy that one of the surface L_s^b carrying a coordinative vacancy and a filled DB is only 2.87 Å away from the C_{CO} atom (see Figure 8).

In Figures 9 and 10 the DOS of the free/chemisorbed CO and the L_s^a/L_s^b−CO COOPs are reported, respectively. If we look at Figure 9 it can be immediately appreciated that the CO HOMO (the 5σ level) is significantly stabilized (∼2 eV) upon

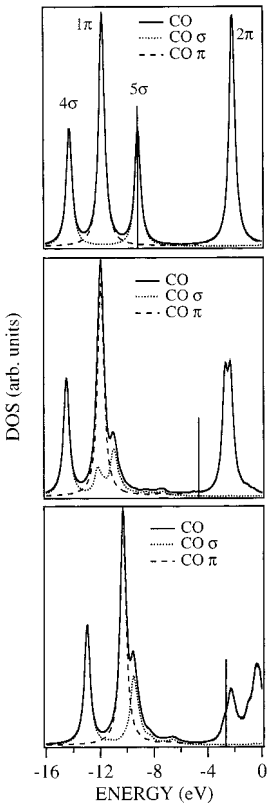

Figure 9. DOS of the free CO (top), PDOS of CO on ^{Al_2O_3}**S3** (middle), and PDOS of CO on ^{Ti_2O_3}**S3** (bottom). σ and π contribution to the DOS/PDOS are also outlined. Vertical bars represent the energy of the highest occupied MO (HOMO).

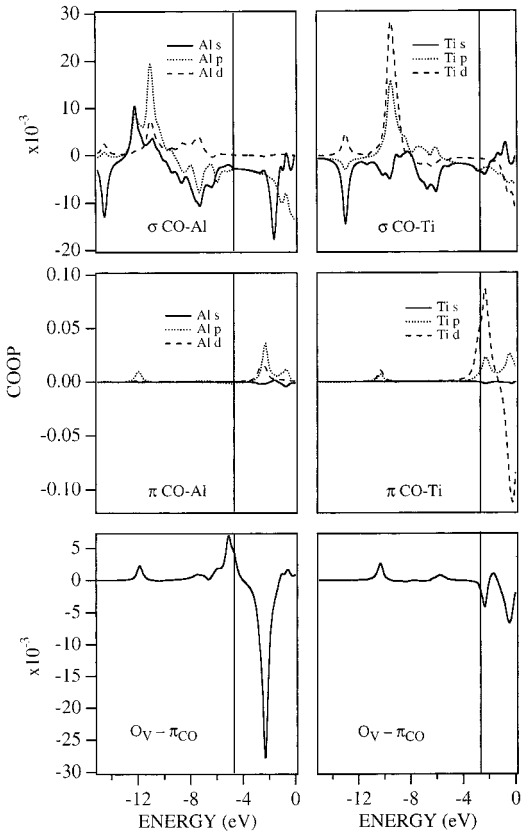

Figure 10. COOP between the L_s^a and CO σ orbitals (top), the L_s^a and CO π orbitals (middle), and L_s^b and CO π orbitals (bottom).

chemisorption, while the energy of CO inner MOs (the 1π and the 4σ orbitals) is perturbed to a very limited extent ($\Delta E_{4\sigma} = 0.24$ eV; $\Delta E_{1\pi} = 0.09$ eV). Moreover, the valence manifold of the chemisorbed CO includes three rather than two peaks having a σ character. A careful inspection of the ^{Al_2O_3}**S3**−CO eigenvectors pointed out that the peak lying at ∼−12 eV, is due to the interaction of the 5σ CO level with the L_s^a 3s AO, while the one at ∼−11 eV derives from the mixing between the 5σ CO level and the L_s^a $3p_z$/3d AOs. The analysis of Figure 10 confirms this scheme, further indicating that the main source of the adsorbate−substrate bonding is a rather weak donation from the CO HOMO into L_s^a 3p/3d AOs.[47] Such a picture is consistent with theoretical outcomes reported in Table 3, which unambiguously indicate that, even if the most relevant contribution to the Al−C bond comes from the electrostatic term, the Pauli repulsion completely offsets this term, thus making determinative, as we found for CO on α-Al_2O_3(0001)[13g] and TiO_2(110)[13e] the orbital contribution.

Inspection of Figure 10 is also useful to understand the origin of the driving force giving rise to the peculiar arrangement of the CO molecule on the $Al_2O_3(10\bar{1}2)$ surface. As a matter of fact, it is well evident that the CO → surface donation is accompanied by a weak, but not negligible, surface → CO back-donation involving the occupied DB of a L_s^b and the adsorbate π^* levels. This interaction is favored, according to Kettle,[46] by the bending of the L_s^a−$\hat{C}$−O BA, which thus provides a reasonable explanation for the geometry of the surface complex.

The comparison of PDOS and COOP for CO chemisorbed on $Al_2O_3(10\bar{1}2)$ and $Ti_2O_3(10\bar{1}2)$ surfaces (see Figures 9 and 10, respectively) coupled to data reported in Tables 2 and 3 reveals significant differences in the interaction of the adsorbate with the two substrates. In particular, the most striking differences are (i) the more negative value of ΔH_{ads}, (ii) the lengthening of the C−O BL, (iii) the dramatic red shift of ν_{C-O} (-179 cm^{-1}),[48] (iv) the negative (-0.10) charge carried by the adsorbate which now behaves as a net acceptor,[50] and (v) the absolute energy position of the CO-based levels.[51]

With specific reference to the first point, the analysis of data reported in Table 3 testifies the leading role played by the ΔE_{int} term in determining heats of adsorption of CO significantly different on the $(10\bar{1}2)$ surface of Ti_2O_3 and Al_2O_3. As a matter of fact, the steric repulsion ($\Delta E_{Pauli} + \Delta E_{elstat}$) of the adsorbate on the former substrate (∼20.1 kcal/mol) is stronger than that on the latter (∼16.5 kcal/mol), thus the more negative ΔH_{ads} of CO on $Ti_2O_3(10\bar{1}2)$ has to be ultimately ascribed to a stronger orbital interaction. The absence of symmetry elements in the ^{M_2O_3}**S**-CO clusters prevents any discrimination between σ and π contributions to ΔE_{int}, but the inspection of Figure 9 can be useful to assess, at least qualitatively, their relative importance. Actually, even if the shape of the PDOS of CO on Ti_2O_3 and $Al_2O_3(10\bar{1}2)$ surfaces is similar,[52] the absolute energy position of peaks related to the CO 4σ, 1π, and 5σ levels is completely different. In particular, for CO on $Ti_2O_3(10\bar{1}2)$, peaks corresponding to the 4σ and 1π MOs are red shifted with respect to the free molecule by 1.3 and 1.5 eV, respectively, while the peak related to the CO 5σ orbital is blue shifted by 0.38 eV. All these evidences are consistent with a bonding scheme where donation (from the CO σ levels into $10\bar{1}2$ d and p empty orbitals) and back-donation (from the $Ti_2O_3(10\bar{1}2)$ VBM into π^* CO levels) play a comparable role.

We already mentioned that the Henrich group[12d] investigated in the middle '80s the interaction of CO with the $Ti_2O_3(10\bar{1}2)$ surface by means of several surface sensitive techniques. The difference spectra they recorded revealed two CO-induced features about 7.5 and 10.7 eV below the Fermi energy (ascribed

to the emission from the CO-based 4σ and $5\sigma/1\pi$ MOs, respectively) and a depopulation of the VBM just below the Fermi energy. Our theoretical findings perfectly match all these data. Actually, the CO-based 5σ and 1π MOs become quasi degenerate upon chemisorption and lie ~7.5 eV below the HOMO energy. Furthermore, the ΔE between the HOMO and the peak due to the 4σ orbital is 10.3 eV. Finally, the involvement of VBM in the Ti → CO back-donation is consistent with the experimentally detected depopulation of this band (in this regard, see in Figure 7 the slight decrease of the Ti−Ti′ COOP upon chemisorption). It is interesting to note that Smith and Henrich[12d] proposed that, for CO exposures $<10^5$ langmuirs, the adsorption process could be "tentatively identified as dissociative on defect site". The significant CO BL lengthening upon chemisorption, coupled to the relevant red shift of the C−O stretching frequency, indicate that, also on the defect free surface and in the zero coverage limit, the C−O bond is significantly weakened.

4. Conclusions

Theoretical results herein reported show that rather small clusters saturated with pseudo-hydrogen atoms are able to realistically mimic the behavior of Al^{3+} and Ti^{3+} Lewis acid sites available on the $(10\bar{1}2)$ surface of Al_2O_3 and Ti_2O_3, respectively. On both surfaces, the CO-surface bonding is characterized by a two-way electron flow, implying a σ donation from the adsorbate into virtual orbitals of surface Lewis acid sites assisted by a back-donation from occupied surface states into CO π^* levels. On $Al_2O_3(10\bar{1}2)$, this back-donation is weak and involves the DB of the L_s^b nearest to the C_{CO}, while on $Ti_2O_3(10\bar{1}2)$, the back-donation is much stronger: it implies the VBM accounting for the Ti−Ti′ ddσ interaction and significantly weakens the C−O bond.

Acknowledgment. Calculations herein reported were carried out on the IBM SP3 system of CINECA (Casalecchio di Reno, Italy). We are grateful to INSTM (Firenze, Italy) for financial support. Finally, it is a pleasure to thank Professor Laura Depero of the University of Brescia (Italy) for insightful discussions.

References and Notes

(1) Linsebigler, A. L.; Lu, G.; Yates, J. T., Jr. *Chem. Rev.* **1995**, *95*, 735.

(2) Botha, S. J. *Mater. Sci. Engin. A* **1998**, *243*, 221.

(3) Henrich, V. E.; Cox, P. A. *The Surface Science of Metal Oxides*; Cambridge University Press: Cambridge, U.K., 1996.

(4) (a) Morin, F. J. *Phys. Rev. Lett.* **1959**, *3*, 34. (b) Zaanen, J.; Sawatzky, G. A.; Allen, J. W. *Phys. Rev. Lett.* **1985**, *55*, 418. (c) Zaanen, J.; Sawatzky, G. A. *J. Solid State Chem.* **1990**, *88*, 8. (d) Mattheis, L. F. *J. Phys.: Condens. Matter* **1996**, *8*, 5987. (e) Catti, M.; Sandrone, G.; Dovesi, R. *Phys. Rev. B* **1997**, *55*, 16122. (f) Nakatsugawa, H.; Iguchi, E. *Phys. Rev. B* **1997**, *56*, 12931.

(5) At high temperature, Ti_2O_3 behaves as a paramagnetic metal with the corundum structure (trigonal Bravais lattice with the D_{3d}^6 ($R\bar{3}C$) space group), and in the temperature range 550−400 K it undergoes a gradual transition to an insulating state with no change in the magnetic and crystallographic symmetry.

(6) Rice, C. E.; Robinson, W. R. *Acta Crystallogr. B* **1997**, *33*, 1342.

(7) Cotton, F. A.; Wilkinson G. *Advanced Inorganic Chemistry*, 5th ed.; Interscience Publishers: New York, 1988.

(8) Luckowsky, G.; Allen, J. W.; Allen, P. *Inst. Phys. Conf. Ser.* **1979**, *43*, 465.

(9) With the exception of a contribution of Guo et al.,[10] dealing with the synthesis of $Ti_2O_3(0001)$ thin films on Mo(110), all the experimental investigation concerning the surface properties of Ti_2O_3 were limited to the $(10\bar{1}2)$ surface.

(10) Guo, Q.; Oh, W. S.; Goodman, D. W. *Surf. Sci.* **1999**, *437*, 49.

(11) Exposed Ti atoms of the $Ti_2O_3(10\bar{1}2)$ surface are involved in a direct ddσ bond with Ti′ atoms of the fourth layer (see Figure 2).

(12) (a) Kurtz, R. L.; Henrich, V. E. *Phys. Rev. B* **1982**, *25*, 3563. (b) Kurtz, R. L.; Henrich, V. E. *Phys. Rev. B* **1982**, *26*, 6682. (c) McKay, J. M.; Henrich, V. E. *Surf. Sci.* **1984**, *137*, 463. (d) Smith, K. E.; Henrich, V. E. *Phys. Rev. B* **1985**, *32*, 5384. (e) Smith, K. E.; Henrich, V. E. *Phys. Rev. B* **1988**, *38*, 5965. (f) Smith, K. E.; Henrich, V. E. *Phys. Rev. B* **1988**, *38*, 9571. (g) Smith, K. E.; Henrich, V. E. *J. Vac. Sci. A* **1989**, *7*, 1967. (h) Kurtz, R. L.; Henrich, V. E. *Surf. Sci. Spectra* **1998**, *5*, 182.

(13) (a) Casarin, M.; Favero, G.; Tondello, E.; Vittadini, A. *Surf. Sci.* **1994**, *317*, 422. (b) Casarin, M.; Favero, G.; Glisenti, A.; Granozzi, G.; Maccato, C.; Tabacchi, G.; Vittadini, A. *J. Chem. Soc., Faraday Trans.* **1996**, *92*, 3247. (c) Casarin, M.; Maccato, C.; Vittadini, A. *Chem. Phys. Lett.* **1997**, *280*, 53. (d) Casarin, M.; Maccato, C.; Vittadini, A. *Inorg. Chem.* **1998**, *37*, 5482. (e) Casarin, M.; Maccato, C.; Vittadini, A. *J. Phys. Chem. B* **1998**, *102*, 10745. (f) Casarin, M.; Maccato, C.; Vittadini, A. *Chem. Phys. Lett.* **1999**, *300*, 403. (g) Casarin, M.; Maccato, C.; Vittadini, A. *Inorg. Chem.* **2000**, *39*, 5232.

(14) The α-$Al_2O_3(0001)$ surface is terminated by a single Al layer, strongly inward relaxed.[15] Each Al surface atom carries three coordinative vacancies and is bonded to three oxide ions, each of them missing a single ligand. As a whole, the number of empty and filled DBs on the α-$Al_2O_3(0001)$ is the same, and the surface is nonpolar.

(15) (a) Ahn, J.; Rabalais, J. W. *Surf. Sci.* **1997**, *388*, 121. (b) Renaud, G. *Surf. Sci. Rep.* **1998**, *32*, 1. (c) Guénard, P.; Renaud, G.; Barbier, A.; Gautier-Soyer, M. *Surf. Rev. Lett.* **1998**, *5*, 321.

(16) Kirfel, A.; Eichhorn, K. *Acta Crystallogr. A* **1990**, *46*, 271.

(17) A cluster atom is chemically complete if it carries a complete shell of nearest neighbours. Obviously, chemically complete cluster atoms representative of the $(10\bar{1}2)$ surface miss a ligand.

(18) *Amsterdam Density Fuctional Package*, Version 1999; Vrjie Universiteit: Amsterdam, The Netherlands, 1999.

(19) (a) Baerends, E. J.; Ellis, D. E.; Ros, P. *Chem. Phys.* **1973**, *1*, 41. (b) te Velde, G.; Baerends, E. J. *J. Comput. Chem.* **1992**, *99*, 84. (c) Fonseca Guerra, C.; Visser, O.; Snijders, J. G.; Baerends, E. J. In *Methods and Techniques in Computational Chemistry*; Clementi, E., Corongiu, G., Eds.: STEF: Cagliari, Italy, 1995; Chapter 8, p 305.

(20) (a) Becke, A. D. *Phys. Rev. A* **1988**, *38*, 3098. (b) Perdew, J. P. *Phys. Rev. B* **1986**, *33*, 8822.

(21) Ziegler, T. *Chem. Rev.* **1991**, *91*, 651.

(22) (a) White, J. A.; Bird, D. M.; Payne, M. C.; Stich, I. *Phys. Rev. Lett.* **1994**, *73*, 1404. (b) Gundersen, K.; Jacobsen, K. W.; Nørskov, J. K.; Hammer, B. *Surf. Sci.* **1994**, *304*, 131. (c) Philipsen, P. T. H.; te Velde, G.; Baerends, E. J. *Chem. Phys. Lett.* **1994**, *226*, 583. (d) Hu, P.; King, D. A.; Crampin, S.; Lee, M. H.; Payne, M. C. *Chem. Phys. Lett.* **1994**, *230*, 583.

(23) Ziegler, T.; Rauk, A. *Theor. Chim. Acta* **1977**, *46*, 1.

(24) Rosa, A.; Ehlers, A. W.; Baerends, E. J.; Snijders, J. G.; te Velde, G. *J. Phys. Chem.* **1996**, *100*, 5690.

(25) Hoffmann, R. *Solids and Surfaces: A Chemist's View of Bonding in Extended Structures*; VCH: New York, 1988.

(26) It can be useful to remember that **B** has the same shape of the cluster adopted by some of us to successfully investigate the UV−vis absorption spectrum of high-purity α-Fe_2O_3 thin films obtained by the sol−gel technique.[27] Furthermore, the unsaturated $[Ti_2O_9]^{12-}$ cluster was adopted by Nakatsugawa and Iguchi[4e] and Évarestov and Panin[28] to investigate the electronic structure of Ti_2O_3.

(27) Armelao, L.; Bettinelli, M.; Casarin, M.; Granozzi, G.; Tondello, E.; Vittadini, A. *J. Phys. Condens. Matter* **1995**, *7*, L299.

(28) Évarestov, R. A.; Panin, A. I. *Fiz. Tverd. Tela* **2000**, *42*, 57.

(29) Guo, J.; Ellis, D. E.; Lam, D. J. *Phys. Rev. B* **1992**, *45*, 3204.

(30) French, R. H. *J. Am. Ceram. Soc.* **1990**, *73*, 477.

(31) Mulliken, R. S. *J. Chem. Phys.* **1955**, *23*, 1833.

(32) The value −1.28 corresponds to the bridging O atoms (O_1), while −1.23 refers to the terminal ones (O_2).

(33) In a series of preliminary calculations on **S1**, **S2**, and **S3** surface ions not directly bonded to saturators (one M atom in **S1**, three M atoms in **S2**, and four M atoms and two O atoms in **S3**, see Figure 3) were allowed to relax. Results pertaining to **S1** and **S2** indicated only minor relaxations, while the computational effort in ^{Ti_2O_3}**S3** resulted out of our computational resources.

(34) Guo, J.; Ellis, D. E.; Lam, D. J. *Phys. Rev. B* **1992**, *45*, 13647.

(35) The $Al_2O_3(10\bar{1}2)$ surface is also known as the $(1\bar{1}02)$ or *R*-cut surface.[36]

(36) Antonick, M. D.; Lad, R. J. *J. Vac. Sci. A* **1992**, *10*, 669.

(37) It is well-known that on low-index faces of oxides CO is always bound to surface L_s^a through the carbon end down. See for instance: Zecchina, A.; Scarano, D.; Bordiga, S.; Ricciardi, G.; Geobaldo, F. *Catal. Today* **1996**, *27*, 403.

(38) Neyman, K. M.; Nasluzov, V. A.; Zhidomirov, G. M. *Catal. Lett.* **1996**, *40*, 183.

(39) The different values refer to different Al−O bond lengths in the cluster representative of the five coordinate Al^{3+}.

(40) The absolute ν_{C-O} values computed for the free and adsorbed CO are 2114 and 2110 cm^{-1}, respectively.

(41) Zecchina, A.; Escalona Platero, E.; Otero Areán, C. *J. Catal.* **1987**, *107*, 244.

(42) Jaeger, R. M.; Homann, K.; Kuhlenbeck, H.; Freund, H.-J. *Chem. Phys. Lett.* **1993**, *203*, 41.

(43) Jaeger et al.[42] pointed out that the topmost layer of their Al_2O_3 substrate consists of oxide ions. Moreover, their data were interpreted by assuming a flat orientation of the molecule with respect to the surface and a large (~4 Å) surface−adsorbate distance.

(44) The effective atomic charge of C (O) atom passes from 0.29 (−0.29) in the free molecule to 0.32 (−0.28) in the one adsorbed on $Al_2O_3(10\bar{1}2)$.

(45) The O_V atoms are those belonging to the fifth layer of the $M_2O_3(10\bar{1}2)$ surface (see Figure 2).

(46) Kettle, S. F. A. *Inorg. Chem.* **1965**, *4*, 1661.

(47) On passing from the clean surface to the one interacting with CO, the L_s^a orbital occupation numbers are modified to a negligible extent.

(48) Even if large, the red shift of the CO streching frequency upon chemisorption on Ti_2O_3 is not particularly surprising because it is known that the C−O stretching band of Ti(III) monocarbonyl complexes such as $[(Me_5C_5)_2Ti(CO)Cl]$[49a] and $[Cp_2Ti(CO)Cl^-]$[49b] lies at 2000 cm^{-1} ($\Delta\nu = -143$ cm^{-1}) and 1950 cm^{-1} ($\Delta\nu = -193$ cm^{-1}), respectively.

(49) (a) Sikora, D. J.; Macomber, D. W.; Rausch, M. D. *Adv. Organomet. Chem.* **1986**, *25*, 317. (b) Murr, N. El; Chaloyard, A. *J. Organomet. Chem.* **1982**, *231*, 1.

(50) The C and O effective atomic charges in ^{Ti_2O_3}**S3**−CO are 0.24 and −0.34, respectively.

(51) Other minor differences regard the slightly longer L_s^a−C BL (shorter than that (2.344 Å) which we computed for CO on $TiO_2(110)$[13e]), the Ti−C−O surface complex less bent that the Al−C−O one, and the O_V−Ti−C BA very close to 180°.

(52) The $\Delta E_{(1\pi-4\sigma)}$ ($\Delta E_{(5\sigma-1\pi)}$) are 2.6 (0.9) and 2.7 (0.7) eV in ^{Al_2O_3}**S3**−CO and ^{Ti_2O_3}**S3**−CO, respectively.